Water Research 161 (2019) 560–569

Contents lists available at ScienceDirect

Water Research

journal homepage: www.elsevier.com/locate/watres

Analysis of suspended microplastics in the Changjiang Estuary: Implications for riverine plastic load to the ocean

Shiye Zhao [a, *, 1], Tao Wang [b], Lixin Zhu [a], Pei Xu [a], Xiaohui Wang [a], Lei Gao [a], Daoji Li [a, **]

[a] State Key Laboratory of Estuarine and Costal Research, East China Normal University, Shanghai, 200062, China
[b] Key Laboratory of Marine, Environment and Ecology, Ocean University of China, Qingdao, 266100, China

ARTICLE INFO

Article history:
Received 26 February 2019
Received in revised form
27 May 2019
Accepted 7 June 2019
Available online 15 June 2019

Keywords:
Plastic debris
Microplastic
Plastic loads
River
Changjiang estuary
East China sea

ABSTRACT

The role of rivers as a major transport pathway for all sizes of plastic debris into the ocean is widely recognized. Global modelling studies ranked the Changjiang River as the largest contributor of plastic waste to the marine environment, but these estimates were based on insufficient empirical data. To better understand the role of rivers in delivering terrestrial plastic debris to the ocean, the spatial and temporal patterns of microplastics (MP) in the Changjiang Estuary (CE) and the East China Sea (ECS) were studied based on surface water samples in February, May, and July 2017. A total of 3225 MP (60–5000 μm) were identified by Fourier-transform infrared (FTIR) spectrometry. MP abundance in July was higher than in February and May due to higher river discharge. Density stratification in CE significantly influenced the surface MP abundances. A temporal accumulation zone within the river-sea interface for plastics was indicated by stations with apparently higher abundances in the river plume. Fibers were the most common MP (>80%) over three months. Small MP (<1000 μm) composed 75.0% of the total plastics on average. The average mass of MP was 0.000033 g/particle, which was two orders of magnitude lower than the empirical mass in literature. Without considering tidal effects, we estimate 16–20 trillion MP particles, weighing 537.6–905.9 tons, entered the sea through the surface water layer of the Changjiang River in 2017. These findings of this study provide reliable information on MP waste in a large river, which should be considered in further studies for estimating the riverine plastic loads.

1. Introduction

Plastic contamination has become one of the most pressing environmental issues. Geyer et al. (2017) estimated that approximately 6300 million tons of plastic waste have been generated worldwide from 1950 to 2015, a fraction of which ultimately enters the marine environment (Geyer et al., 2017). Plastic waste in the global ocean is estimated to be more than 150 million tons (Neufeld et al., 2016). Roughly 80% of ocean macroplastic debris (>5 mm) have terrestrial origins (Dauvergne, 2018), while ~98% of microplastics (MP, < 5 mm) are from land-based sources (Boucher and Friot, 2017). Macroplastics have been the subject of environmental studies for some time. However, in the past decade, the focus has shifted on the ubiquitous MP, which are made up of small plastics derived from the fragmentation of macroplastics and are of microscopic size (Galloway and Lewis, 2017). Rivers are considered as an important vector for the transport of different types of debris into the sea (Rech et al., 2014; Sadri and Thompson, 2014). A better understanding of the role of rivers in transporting plastics into the ocean is crucial for clarifying the sources, pathways, and mass balance of ocean plastics.

Recently, plastic debris loads of global rivers into the ocean were modeled based on global mismanged plastic waste. Annually, 1.15–2.41 million tons of plastic waste currently enter the ocean from rivers worldwide, with >74% of emissions occurring between May and October (Lebreton et al., 2017). Similarly, Schmidt et al. (2017a,b) estimated that 0.41–4.0 million tons of land-based plastic debris are transported by rivers into the ocean each year (Schmidt et al., 2017a). Furthermore, both the above studies noted that the top polluting rivers, mostly located in Asia, accounted for 67%–94% of the global plastic load. Based on their caculations, the Changjiang River was regarded as the largest contributor worldwide, delivering 0.15–0.33 million tons of platic waste (both

* Corresponding author.
** Corresponding author.
E-mail addresses: shiyezhao@gmail.com (S. Zhao), daojili@sklec.ecnu.edu.cn (D. Li).
[1] Present Address: Harbor Branch Oceanographic Institute, Florida Atlantic University, Fort Pierce, Florida 34946, United States.

https://doi.org/10.1016/j.watres.2019.06.019
0043-1354/

macro- and micro-plastic) per year into the adjacent East China Sea (ECS) (Lebreton et al., 2017; Schmidt et al., 2017a). However, estimates from both studies are uncertain due to the sparse and hetergeneous datasets. Data from different studies on riverine MP that were compiled and analyzed by the models vary significantly, which is likely attributed to the sampling design, collection devices, analysis methods, and report units. For instance, no more than three or four consecutive measurements were found in the dataset used by Schmidt et al. (2017a).

As one of the largest rivers in the world, MP in the Changjiang Estuary (CE) is poorly studied. Zhao et al. (2014) filtered water samples (12–20 L per sample) through 32 μm sieves and reported that the mean suspended MP abundance in the CE (Yangtze Estuary) was 4137 n/m^3 (Zhao et al., 2014). However, this estimate was based on a sole sampling campaign in July, and the lack of chemical identification of the suspected plastic particles in this study inevitably led to significant errors (Hidalgo-Ruz et al., 2012). Luo et al. (2019) recently studied MP pollution in the CE and the ECS by filtering 5 L surface water through 20 μm nylon filters and reported the mean abundance of MP in the estuary and coastal water to be 900 n/m^3 (Luo et al., 2019). By studing the microplastic at 15 sites along the middle and lower reaches of the Yangtze River (Changjiang River), Xiong et al. (2019) obtained a range of MP abundance from 1.95×10^5 to 9.00×10^5 items/km^2. They also suggested that a considerable amount of MP from the large river cathments did not reach the sea. In the present study, a much larger number of surface water samples (100 L per sample) were collected from the CE and EST during three cruises in different seasons (winter, spring, and summer). The spatial and temporal features of floating MP (60–5000 μm) abundance, distribution, and composition in the studied region were analyzed, which could assist in identifying the spatial and seasonal patterns of plastic transport fluxes from the land to sea and support the implementation of cost-effective monitoring and source mitigation efforts. Furthermore, we compared the overall MP (300–5000 μm) abundance in the CE with global estuaries and roughly estimated the plastic load passing through CE into the ESC. Our results should improve the assessment of plastic load from rivers to the sea.

2. Materials and methods

2.1. 1. sampling

MP were collected during three research cruises (15–28, February 2017; 5–23 May 2017, and 18 July–3, August 2017) onboard the R/V Run Jiang No. 1 in the CE and the ECS (Fig. 1). Detailed information of the studied region and sampling sites is provided in the supplementary data and the excel sheet. Water samples were collected using a screw pump, which was deployed at around 30 cm depth on the front port side of the ship. For each sample, 100 L water was pumped into a high-density polyethylene (HDPE) tank with a metal tap at the bottom. All samples within the CE were taken during the ebb phase only. The collected waters were filtered through a stainless-steel sieve (pore size: 60 μm). The retained materials on the sieve were flushed into clean 250 mL poly-tetra-fluoroethylene bottles with Milli-Q water. Samples were stored at 5 °C prior to analysis. One sample (100 L waters) was collected at each sampling site during the February cruise, while three replicates (100 L × 3) were sampled during the May and July cruises. Detailed information of the samples is listed in Table S1. The profiles of temperature, salinity, and density at each station were measured with a conductivity, temperature, and depth (CTD) device (Sea-Bird Electronics-25; Bellevue, WA, USA).

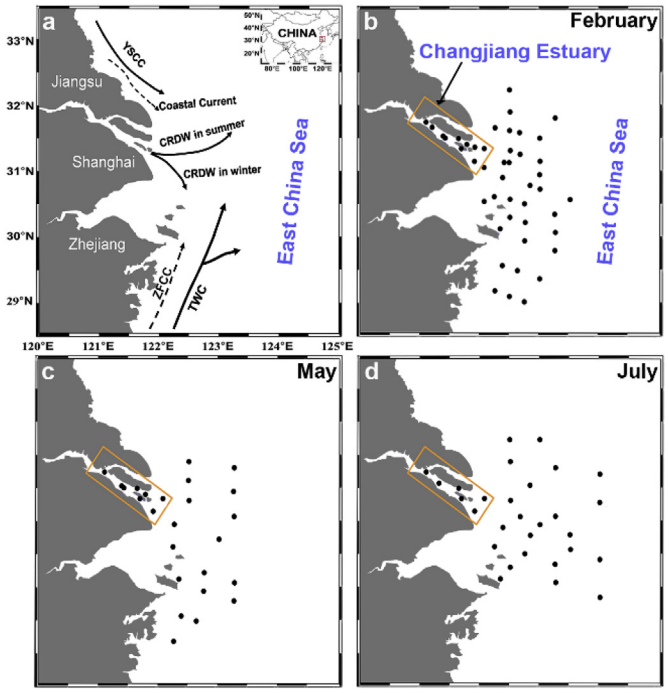

Fig. 1. Map showing the main currents (a) and sampling sites (b. February, c. May, d. July) in three months. TWC, Taiwan Warm Current; YSWC, Yellow Sea Warm Current; ZFCC, Zhejiang-Fujian Coastal Current; YSCC, Yellow Sea Coastal Current; CDW, Changjiang diluted water. The orange boxes show the sampling stations within the CE.

2.2. Laboratory analyses

In the lab, samples were transferred into clean glass beakers and digested with 30% H_2O_2 solution at 60 °C to eliminate organic matter. This step was repeated if necessary until the solution was clear in appearance. The contents were then filtered through 0.45 μm Sartorius filters (47 mm diameter). An individual filter was stored in a glass Petri dish and examined under a stereo microscope (LeicaM165 FC at magnification 160 ×) based on summarized criteria from previous research (Nor and Obbard, 2014; Zhao et al. 2014, 2016). A detailed protocol is provided in the supplementary data. Suspected particles were marked with red circles on the filter. The particles were then photographed and measured for the largest dimension using the built-in Leica Application Suite X software. Particles within the range of 60–5000 μm were enumerated. Based on morphology, the suspected particles were categorized into fiber, film, and fragments. Finally, all particles were analyzed using micro-Fourier transform infrared (FTIR) spectroscopy (Bruker LUMOS, Germany) in attenuated total reflectance (ATR) mode. Each scan was accumulated as the average of 32 scans in the spectral range of 600–4000 cm^{-1} at a resolution of 4 cm^{-1}. Three replicate ATR-FTIR spectra were acquired on different spots of each particle. Each spectrum was compared against a database from Bruker to verify the polymer type. Matching spectra with a quality index ≥70 were accepted.

2.3. Contamination prevention

Utmost precautions were taken to prevent sample contamination throughout the entire research process. Prior to use, the HDPE graduated tanks and steel sieves were thoroughly washed with Milli-Q water and then double-covered with tinfoil. In the field, prior to their first use at each sampling site, all containers (e.g., the HDPE tanks and PTFE bottles) were rinsed with 60 μm filtered *in*

situ seawater. In the laboratory, the measurements reported by (Zhao et al., 2017) were employed. All of the liquid reagents and media were filtered through 0.45 μm glass filters (Whatman, GF/F). Glassware (such as beakers, filtration system, glass filters, Petri dishes, tinfoil, and Pasteur pipettes) is recommended for use as much as possible during the entire procedure and should be rinsed with Milli-Q water and heated at 450 °C for 8 h to combust any organic materials. During the procedure, the clean glassware should be covered with combusted tinfoil wherever and whenever possible. Steel tweezers were washed with Milli-Q water and sterilized under a flame prior to use. All sample handling was carried out under a clean laminar flow cabinet. Personal protective ware, such as nitrile gloves and cotton lab coats, were worn during the laboratory activities. Air was drawn through three clean filters (0.45 μm, Sartorius) during the plastic separation in the lab to determine the potential airborne particle contamination. A mixture of filtered 30% H_2O_2 solution and Milli-Q water in three combusted glass tubes was run through the whole processing procedure as process blanks.

2.4. MP load through the CE

The yearly MP mass in the surface layer (around 30 cm depth) passing through the CE was estimated using the following equation:

$$Load_{CE} = \sum_{i=1}^{4} (C_i \times Mass_{micro} \times Discharge_i \times Discharge_{ratio-i} \times 3 \div 10^6)$$

Where $Load_{CE}$ (tons/year) is the annual plastic flux input to the ocean, a sum of plastic masses of the four seasons (spring, summer, fall and winter). The symbol i represents the four seasons. C_i is the mean MP concentration (n/m^3) of each month in corresponding season. Based on the river discharge and rainfall, the datasets sampling in February, May and July represent the MP abundances in the winter, spring and summer of the year. Three measured MP concentrations were designed as the concentration in the fall, representing the low, midpoint, and high values (Table 1). $Mass_{micro}$ is the averaged MP mass per particle (0.000033 g). The average mass of MP was generated by measuring three subsamples of randomly selected plastic items from the CE. For each replicate, 100 identified plastics composing of 80 fibrous and 20 non-fibrous particles were selected under the stereo microscope (LeicaM165 FC) and put on small pieces of pre-weighed filter disc to reduce tare weight as low as possible. $Discharge_i$ (m^3/month) was taken as the monthly averaged discharge of each season in Changjiang River, which were obtained from Yangtze River Sediment Bulletin (The Changjiang Water Conservancy Committee, 2017). $Discharge_{ratio-i}$ is the proportional discharge rate through the top 30 cm. It is under the assumption the discharge rate is constant throughout all depths, which we aware is an over simplification. $Discharge_{ratio-i}$ was calculated from the depth (around 30 cm) divided by the average water depth of the sampling stations in three months (Miller et al., 2017). The ratio is under the assumption that the discharge is constant throughout all depths. All the parameters used to estimate plastic loads were shown in Table 1.

2.5. Statistical analysis

The Kruskal-Wallis test was used to analyze multiple comparisons. If the test indicated significant differences, pairwise comparisons were performed using the Wilcoxon test. In all tests, an alpha level of 0.05 was used. Data are reported as mean ± standard deviation (SD). SURFER 11 (Golden Software LLC, Golden, CO, USA) was used to draw contour lines based on kriging (interpolation). The strength of stratification is indicated by the density difference ($\Delta\rho$) between the bottom and surface of each station.

3. Results and discussion

3.1. MP abundance

No plastic particles were present in our process blanks. But natural material-based fibrous particles (either cotton or rayon, semi-synthetics) were found on the air sucked filters (Fig. S1), which were not enumerated in results of this study. Plastics were found in 99% (205/207) of all samples. A total of 3225 MP (60–5000 μm) were confirmed by ATR-FTIR. The overall mean MP concentrations in CE and ECS were 157.2 ± 75.8 n/m^3 and 112.8 ± 51.1 n/m^3, respectively. MP abundance in the CE was over 25 times lower than that (4137.3 ± 2461.5 n/m^3) measured by (Zhao et al., 2014), although both studies used pumps to collect samples. This disparity may be primarily attributed to the lack of validation of the chemical matrix of the plastic-like particles using complementary methods (e.g., spectroscopic and thermo-chemical methods) by Zhao et al. (2014). The plastic identification by Zhao et al. (2014) was exclusively based on visual inspection using light microscopy. Visual identification alone has been reported to result in a high misidentification rate, ranging from 20% (Eriksen et al., 2013) to 70% (Hidalgo-Ruz et al., 2012). MP concentrations in the sediment samples from similar locations in Europe showed ca. 100-fold differences between the visual identification data and FTIR data (Claessens et al., 2011; Liebezeit and Dubaish, 2012). Furthermore, the visual identification error rate increases with decreasing particle size (Löder et al., 2015). All particles in this study were identified by ATR-FTIR, guaranteeing the accuracy of polymer identification. Additionally, smaller sampling volumes, 20 or 12 L per sample in 2014, could result in highly variable concentrations (Lusher et al., 2014; Tamminga et al., 2018). Recently, Luo et al. (2019) reported the average MP abundance in both the CE

Table 1
The yearly microplastic load estimations of Changjiang River in 2017.

Season	MP abundance per month (n/m^3)	Mean discharge (m^3/month)	$Discharge_{ratio}$	Counts in the season	Mass (tons)
Spring	45.4	741.5×10^9	0.022	2.3×10^{12}	112.3
Summer	122.8	1206.2×10^9	0.021	9.5×10^{12}	476.0
Winter	83.0	396.8×10^9	0.022	2.2×10^{12}	109.8
Fall-low	45.4	798.1×10^9	0.021	2.3×10^{12}	76.9
Fall-midpoint	83.0	798.1×10^9	0.021	4.3×10^{12}	140.5
Fall-high	122.8	798.1×10^9	0.021	6.3×10^{12}	207.9
Total-low				16.3×10^{12}	537.6
Total-midpoint				18.2×10^{12}	601.3
Total-high				20.3×10^{12}	905.9

Notes: The averaged abundances in February, May and July were used as the mean MP abundances for each month within the winter, spring and summer.

and EST to be 900 n/m^3, which is higher than our results in the CE (157.2 n/m^3) and ECS (112.8 n/m^3). The 20 μm filters employed by Luo et al. (2019) in comparison to 60 μm in our study might primarily contribute to this difference. The temporality of plastic pollution levels also contributed to this difference. Seasonal conditions play a significant role in the transportation of litter by rivers to the sea and lead to several orders of magnitude variation between plastic abundances at different periods (Lebreton et al., 2017; van der Wal et al., 2015; Vianelloa et al., 2015). The concentration of the CE in this study was averaged from the data in February, May, and July 2017, spanning the lower to higher discharge rates of the Changjiang River. However, the concentration in the CE in Zhao et al. (2014) was based only on a single sampling in July, which might be largely biased in comparison to the abundance of MP in the CE in this study. This emphasizes that long-term, systematic monitoring research for plastic litter items in the riverine environment is necessary to obtain more realistic and representative abundances of plastic debris in the future.

The average concentration in the ECS (112.8 ± 51.1 n/m^3) was three orders of magnitude larger than a previous study (0.167 ± 0.138 n/m^3) identified using 333 μm manta net samples (Zhao et al., 2014). Similarly, MP abundances in the ECS were several orders of magnitude greater than other studies that used net trawls with various mesh sizes as the sampling device (Table S2). The bulk water sampling methods utilized in current studies have mainly contributed to this large disparity. To determine the influence of variable sampling techniques, net-based and bulk sampling approaches have been compared in several studies. In the South China Sea, the MP concentration (0.045 ± 0.093 n/m^3) of the 333 μm bongo net samples was four orders of magnitude lower than that of pumping waters samples (2569 ± 1770 n/m^3) at a depth of 0.5 m (Cai et al., 2018). (Di Mauro et al., 2017) also found that MP concentrations (20, 000 ± 6000 particles/m^3) in Niskin samples collected at approximately 1 m, 5 m, and 10 m from the sea surface were several orders of magnitude greater than either bongo (4.6 ± 0.8 n/m^3) or neuston nets 8.6 ± 2.0 (n/m^3) at sampling sites in the northern Gulf of Mexico. The contamination level determined by manta trawling was 0.07 ± 0.02 n/m^3 in contrast to that of 1030 ± 800 n/m^3 by bulk sampling from three depths (0.5 m, 2.0 m, and 5.0 m) in the South Funen Archipelago, Baltic Sea (Tamminga et al., 2018). Two factors likely explained the order of magnitude disparity in MP concentrations between the bulk water and the net-based samples. First, the detection limitation of the plastic by net sampling is dependent on the mesh size selected. As expected, a smaller mesh size can retain considerably more plastics than a larger mesh size. Song et al. found that MP abundance in 50 μm hand-net samples (1443 ± 3353 particles/m^3) was significantly larger than in manta trawling samples (47 ± 192 particles/m^3) (Song et al., 2014). MP abundance in coastal Swedish waters in 80 μm and 450 μm mesh samples varied by up to six orders of magnitude (Norén, 2007). A typical manta trawl cannot sample MP particles smaller than 300 μm, resulting in the omission of smaller-sized fractions. Second, smaller and larger particles can be either forced aside from the net opening or squeezed out through the mesh. For example, particles (e.g., fibers) with lower aspect ratios can easily pass through the net by aligning themselves with the flow direction (Setälä et al., 2016). Particle size spectrum theory in the marine environment predicts that abundance increases with decreasing particle size (Sheldon and Parsons, 1967). On average, 29.4% of MP particles in our study were smaller than 0.3 mm (Fig. 6abc, Table S3). This suggested that studies extrapolating neuston tow data to worldwide abundances (Cózar et al., 2014; Eriksen et al., 2014) may similarly underestimate MP abundance in the sea.

3.2. Temporality of MP abundances

MP abundances in the CE and ECS varied considerably across the three months (Fig. 2, Table S1). MP concentrations in the CE were apparently different among the different months as well as that in the ECS (Kruskal–Wallis test, $p_{CE} = 4.10 \times 10^{-4}$, $p_{ECS} = 1.19 \times 10^{-5}$). The concentrations in July of the CE and ECS were apparently higher than those of the other months. Influenced by the East Asian monsoon, the studied area in July 2017 was characterized by the highest level of rainfall among the three sampling seasons, resulting in an increased river flux into the estuary, which likely explained the seasonality of MP abundance. Mismanaged waste generated in the river basin could migrate toward the estuarine portion following the river flow. Plastic litter retained in the adjacent areas around the estuary can be flushed into the waterways more frequently in the rainy season than the dry season, eventually entering into the adjacent sea (Lima et al., 2014; Moore et al., 2002; Zhao et al., 2015). This distinct seasonality in MP abundance emphasizes that temporal variations must be also considered when monitoring the levels of plastic pollution within a region that has high seasonal variations in rainfall. An overestimation of 53.9% in the CE and 55.7% in the ECS would occur if the average abundance of MP in this study was calculated solely from the data obtained in July.

3.3. Patchy distribution of MP

No differences were found between MP abundances in the CE and ECS of each month (Wilcoxon test, February $p = 0.99$, May 0.73, July 0.66). However, the abundances fluctuated highly among the sampling sites within each month. The average MP abundance of each site ranged from 20.0 to 290 n/m^3 in the CE and 10.0 to 647.6 n/m^3 in the ECS (Fig. 3). A high spatial heterogeneity of MP abundance on a smaller scale has been shown previously (Goldstein et al., 2013). Unexpectedly, the highest MP concentrated sites (sites #A2-5, #A8-2, #A8-4 in February; #A9-4, #A10-3, #A11-1 in

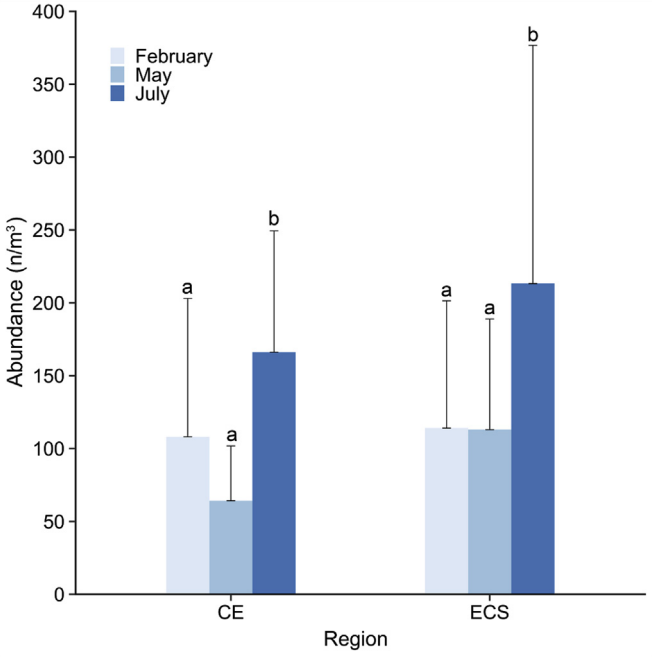

Fig. 2. MP abundance across the sampling regions (a) and months (b). Bars sharing the same letter are not significantly different.

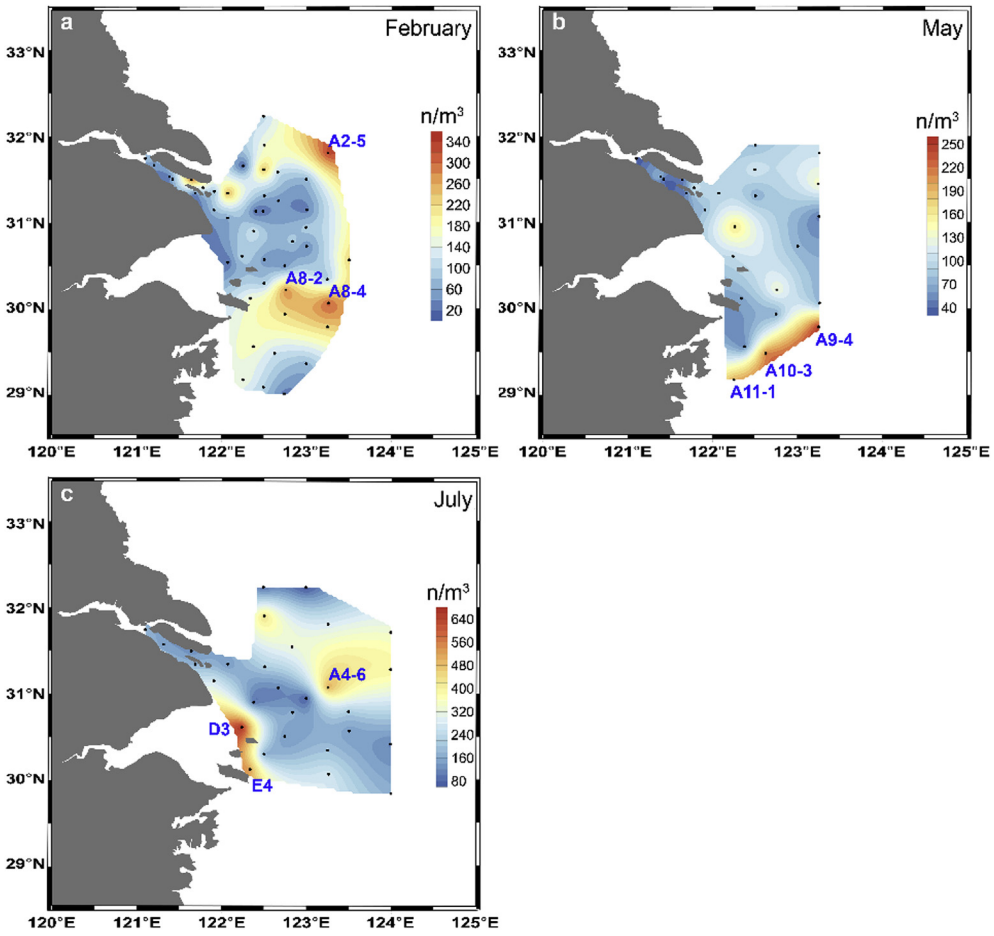

Fig. 3. Spatiality distribution of MP in the CE and ECS in the three months (a. February, b. May, c. July). High-abundance sites in the ECS are indicated in blue letters.

May; #A4-6, #D3, #E4 in July, Fig. 3) in this study were all located in the ECS and not in the internal estuary (CE), which is inconsistent with a previous study that reported higher MP abundances in the estuary than in the ECS (Zhao et al., 2014). The patchiness in the floating MP distribution is probably related to the following factors: 1) plastic particles display an increasing frequency distribution skewed toward smaller size classes in many studies (Cózar et al., 2014). MP size at sites with higher abundance in the ECS were considerably smaller than those from estuarine sites (Fig. 4). The fast flux of smaller-sized MP within limited distances from the coast, depending on the fast fragmentation of terrestrial plastic debris, may contribute to this size disparity (Pedrotti et al., 2016). 2) Plastics at the sea possess more variant origins. Due to the high dispersion, MP at the sea may come from both the land and sea. In the ECS, the northward Kuroshio Branch Current (KBC) and Taiwan Warm Current (TWC) were steady and may transport floating plastic litter to our study area. The Kuroshio current system has been thought to deliver plastic waste from Asia to the "Great Pacific Garbage" (Lebreton et al., 2018). Due to the instantaneous sampling in the current study, other factors (e.g., tidal currents, wind, eddies, river flow, vertical mixing, and wave action) may also contribute to the surges in MP abundance at some sampling sites, resulting in temporal patches for floating MP (Schmidt et al., 2017b; van der Hal et al., 2017).

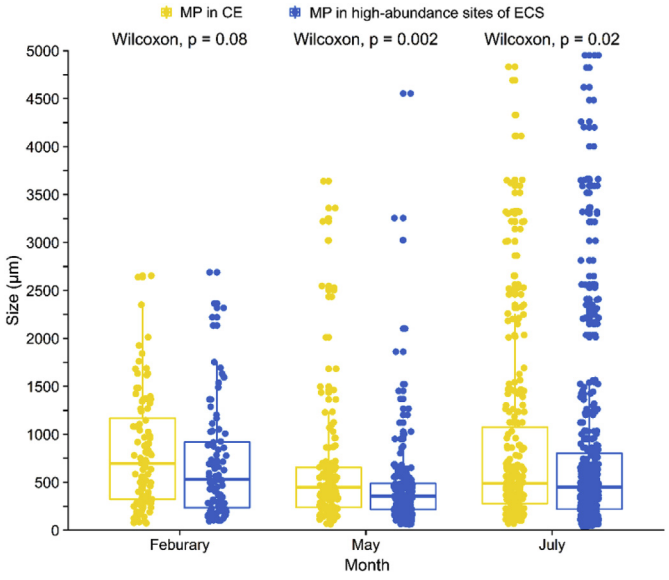

Fig. 4. Size distribution of MP between sampling sites in the CE and high-abundance sites in the ECS. A Wilcoxon test was employed to compare MP sizes between the sites.

3.4. Characteristics of MP

MP size in this study ranged from 60 to 4953 μm and displayed an asymmetrical frequency distribution skewed toward smaller size classes (Fig. 5abc). Particles smaller than 300 μm accounted for 29.4% of the total number, ranging from 21.8% to 30.6% in CE and

ECS across the different months and regions (Fig. 5abc and Table S3). Furthermore, MP < 1 mm, a size-specific loss of floating plastic in the open ocean (Cózar et al., 2014), comprised 75.0% of the total number and varied from 68.2% to 86.3%. The large fractions of smaller-sized MP corroborated that of studies based on the commonly used net trawl sampling technique, which might miss considerable plastic debris in the surface waters and contribute considerably to the missing plastic in the global ocean (Cózar et al., 2014).

The mean size of MP in the CE varied significantly over the three sampling months (Kruskal-Wallis test, $p = 4.1 \times 10^{-3}$), as well as that in the ECS (Kruskal-Wallis test, $p = 1.3 \times 10^{-11}$). The particle size in May was apparently smaller than the measurements in February and July (Wilcoxon test, $p = 1.0 \times 10^{-14}$, 7.7×10^{-6} in the ECS; $p = 0.01$, 0.01 in the CE, Fig. 5d). Though plastics are designed to be persistent, physical factors (e.g., wave action and wind) and UV light enhance their fragmentation in the environment depending on the exposure time (Andrady, 2011). However, the short interval between samplings in this study may not have allowed the plastics to become sufficiently photo-degraded. This temporal pattern in mean size could be largely ascribed to heavy rainfall during the wet season. At the beginning of the wet season (May), MP in the Changjiang catchment, which had become brittle and fragmented into smaller-sized particles due to multiple factors (e.g., UV, wind, exposure to air), were probably flushed into the CE and the adjacent ECS. A similar result was reported by Gündoğdu et al. (2018), who found that the average size of the floating MP in the Mersin Bay decreased from 2.37 mm in the pre-flood period to 1.13 mm in the post-flood period (Gündoğdu et al., 2018).

Among the morphology categories, fibrous particles were the most common (Fig. 6a), accounting for 77.8–91.6% (CE) and 83.4–91.5% (ECS) of all particles in the three months, followed by film [5.6–17.4% (CE) and 5.8–15.9% (ECS)], and fragments [0–6.6% (CE), 0–10.2% (ECS)]. The dominance of fibers in our study was consistent with previous studies (Enders et al., 2015; Gallagher et al., 2016; Lahens et al., 2018; Zhao et al., 2014), and it has been suggested that the fiber is of land-based origin (Browne et al., 2011). Experimental studies found that >1900 fibers could be shed per machine wash, and over 700, 000 fibers could be released from a mean 6 kg wash load of acrylic fabric (Napper and Thompson, 2016). These fibers within the waste effluent from washing machines will be transported to sewage treatment plants. Some of these fibers are able to pass through the screens present at sewage treatments and enter into the aquatic environment (Dris et al., 2015; Napper and Thompson, 2016). Shanghai city, located within the CE, is currently the most developed (approximately 370 billion USD of gross domestic product in 2015) and populated (ca. 24.15 million inhabitants) city in China (Shanghai Statistical Yearbook, 2016). It has been demonstrated that the dense population and economic development in mega-cities contributes to MP

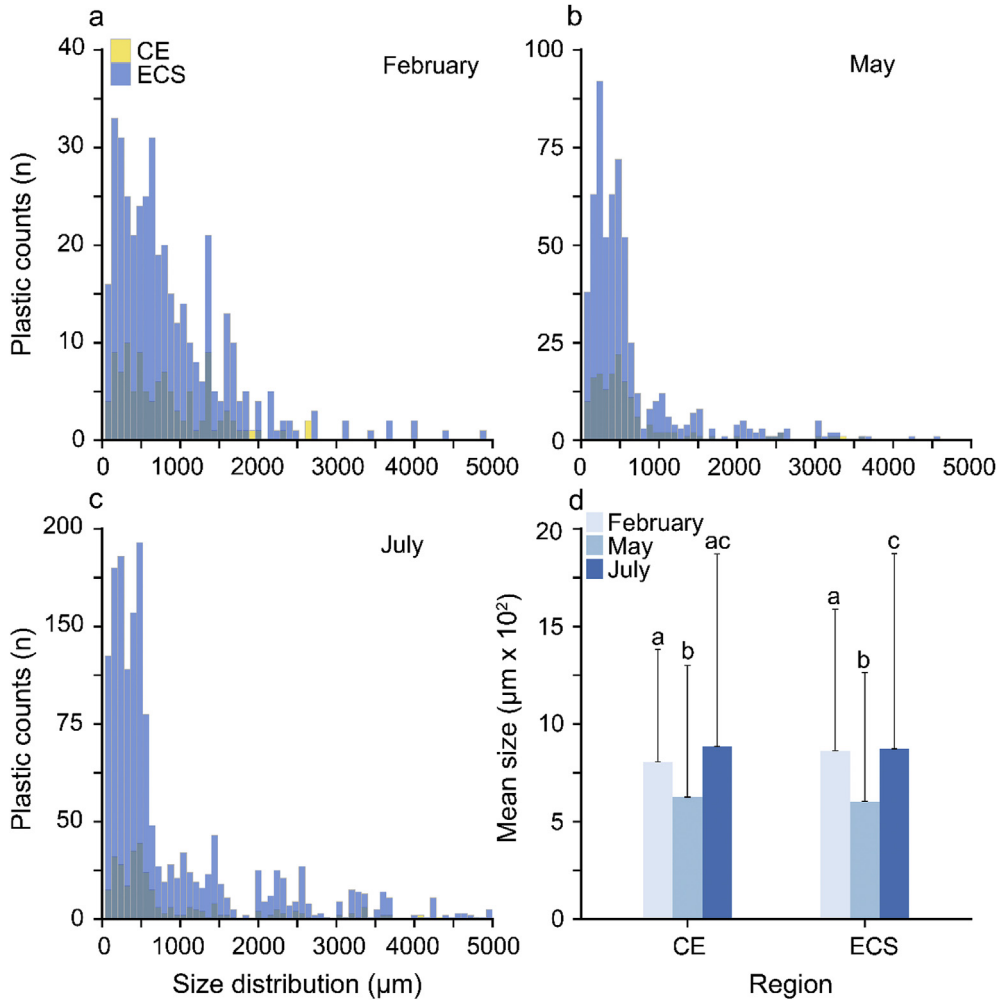

Fig. 5. Size distribution in three months (a. February, b. May, c. July), and the average size of MP identified in two sampling regions (d). Bars sharing the same letter are not significantly different.

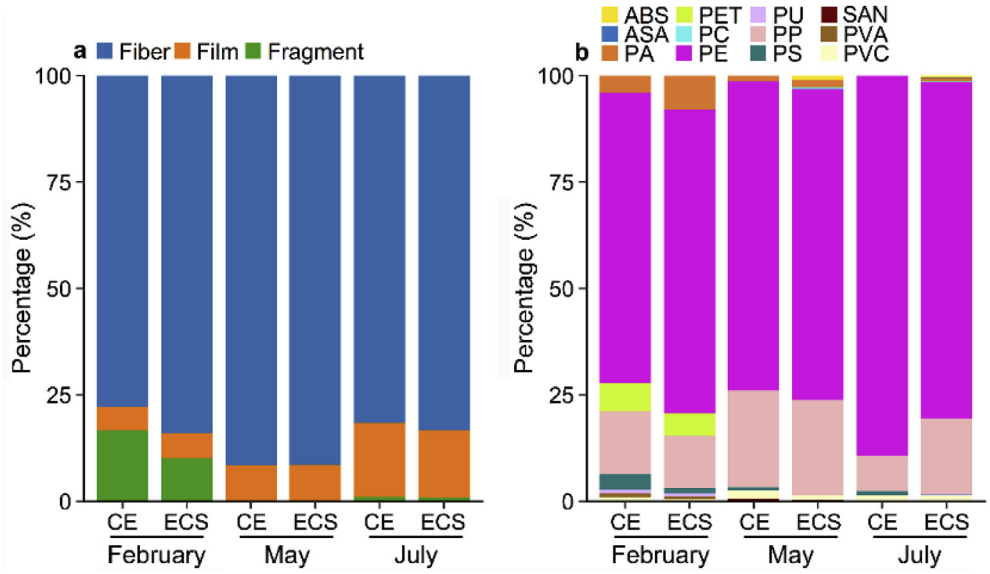

Fig. 6. Morphology (a) and polymer types (b) distribution of the floating MP in the CE and ECS.

contamination in the aquatic environment (Lahens et al., 2018; Peng et al., 2018). A recent study by Bai et al. (2018) corroborated this notion. They reported that a coastal sewage plant in Shanghai could release 1.456 trillion MP per day into the CE, 74.44% of which were fibers (Bai et al., 2018). Luo et al. (2019) also reported a high proportion of fibers (66%) in the water samples from the CE (Luo et al., 2019). Additionally, atmospheric fallout is also a way for land-originated fibers to move into the aquatic environment (Dris et al., 2016). Generally, microbeads found in the environment are mainly sourced from cosmetics, such as facial cleaners, body washes, and toothpastes (Napper et al., 2015), which are produced in the size range of 74–250 μm. Although microbeads occupy the lower end of the 0.1–5000 μm scale, they should have been retained by our 60 μm stainless steel sieve during the filtering of water samples in the field. Unexpectedly, no microbeads were found in our study. Compared to other morphologies (film and fragments), smaller microbeads with high surface area to volume ratios are prone to fouling and sink rapidly (Fazey and Ryan, 2016), as indicated by two field studies. By analyzing sediment samples in the CE and ECS (Peng et al., 2017), found that microbeads accounted for 1% of the total MP counts (n = 570), whereas Peng et al. (2018) reported that spherical particles constituted 89.0% of MP in the sediments of the Huangpu River, which is the last tributary of the Changjiang River and flows through Shanghai City into the South Branch. These studies suggest that the microbeads sank into the sediments of the Huangpu River before entering the CE.

Twelve polymer types were identified using micro-FTIR (Fig. 6b). Polyethylene (PE) and polypropylene (PP), the most widely used polymer types in non-fiber plastic products (Geyer et al., 2017), comprised the majority of polymers in this study. Polyester (PET) accounts for over 50% of global fiber production (Hernandez et al., 2017). It accounted for 6.5% and 5.3% of the particles in the samples in the CE and ECS in February 2017. However, PET was absent in the samples in May and July 2017, although this does not necessarily indicate its absence at these sites. Polyamide (PA, nylon) is also one major component of fiber production and is extensively used as a material for fishing gear manufacturing (Sala et al., 2018). Styrene acrylonitrile (SAN), polystyrene (PS), polyvinyl chloride (PVC), polycarbonate (PC), polyurethane (PU), polyvinyl alcohol (PVA), acrylate styrene acrylonitrile (ASA), and acrylonitrile butadiene styrene (ABS) have been frequently identified in Asian seawater samples (Cai et al., 2018; Lahens et al., 2018; Ng and Obbard, 2006; Song et al., 2015; Tsang et al., 2017; Xu et al., 2018; Zhao et al., 2015).

3.5. Comparing plastic loads between CE and global estuaries

Nets with mesh sizes of 333 or 335 μm are the most commonly employed samplers in aquatic MP research (Hidalgo-Ruz et al., 2012; Zhao et al., 2018). To better understand MP contamination in the CE, comparisons between our results and those in other estuaries that also depended on bulk water samples are important. The abundance (mean: 79.4 ± 60.8 n/m^3; a range of 10–260 n/m^3) of MP (300–5000 μm) in the CE was calculated by removing the smaller-sized fraction (60–300 μm). In general, the MP (300–5000 μm) abundance of the CE was in the upper range of concentrations measured in other estuaries (Fig. 7). The MP abundance (300–5000 μm) in the CE in this study is comparable to that (335–5000 μm, 83.5 particles/m^3) reported in the surface water in the Strait of Juan de Fuca, Salish Sea (Hansen, 2016). The high pollution level of MP in the CE could be explained by the close proximity of the most densely populated area worldwide, where effluents containing MP inputs from the surrounding large wastewater treatment plants enter into the aquatic environment. The values reported in Charleston Harbor (6600 particles/m^3) and Winyah Bay (30,800 particles/m^3) (Gray et al., 2018) were two to three orders of magnitude higher than that in our study and could mainly be attributed to the smaller sieve size (63 μm) used to process the sea surface microlayer samples (4 L/sample). Inconsistent methodologies among the current literature must be considered when comparing these studies.

Based on MP abundance (60–5000 μm), we estimate 16–20 trillion MP particles, weighing 537.6–905.9 tons, annually entered the sea through the top water layer of the Changjiang River (Table 1). Based on the model and datasets used by (Lebreton et al., 2017), the low-, mid- and high MP loads of the Changjiang River were 0.9×10^5, 1.0×10^5, 1.5×10^5 tons/year, which were 2-3 orders of magnitude higher than our estimates. This striking disparity between the two studies could mainly be attributed to the different MP mass values empolyed. An empirical average mass of MP (0.003 g/particle) used by Lebreton et al. (2017) is almost 2 orders of magnitude higher than our measured mass (0.000033 g/particle).

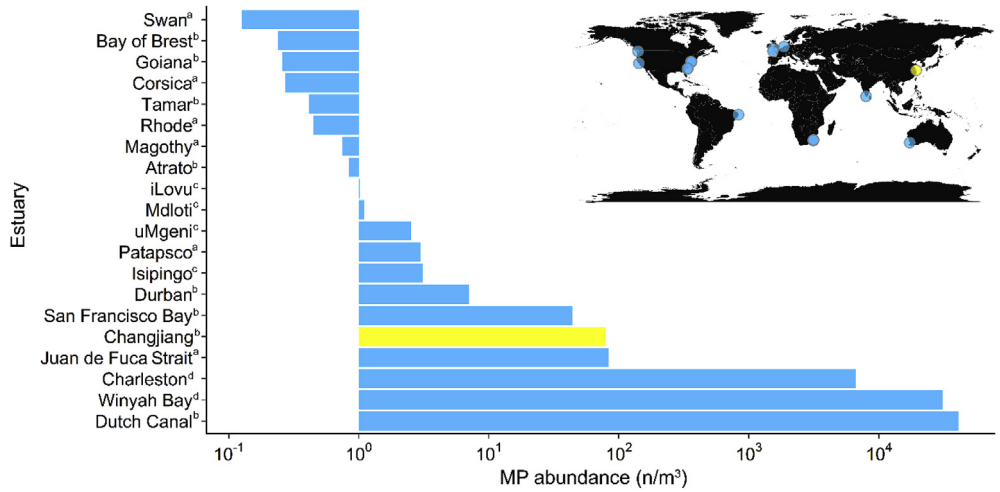

Fig. 7. Comparison of floating MP abundance (mean value) between the CE (the yellow bar) and those (blue bars) in other estuaries worldwide. The map displays the approximate locations of this study (the yellow dot) and other studies (blue dots). The superscript letters indicate net mesh size: a, 333 μm; b, 300 μm; c, 250 μm; d, 63 μm.

Lebreton et al. (2017) calculated this mean mass based on the numerical concentrations and mass reported by Eriksen et al. (2014). In their study, the abundance and weight of MP was estimated by counting and weighting the MP captured by the 330 μm neuston nets. However, the composition of MP morphologies (e.g., fibers and fragments) was not provided (Eriksen et al., 2014). MP data by Zhao et al. (2014), which was composed of 79.1% fiber, was used to estimate the plastic flux of Changjiang River by Lebreton et al. (2017). In present study, over 80% of MP were fibrous particles (Fig. 6a). The similar fiber proportions in both studies implied the empirical MP mass averaged by the oceanic MP particles was not applicable to riverine samples and Lebreton et al. (2017) largely overestimated the MP loads of the Changjiang River. Furthermore, this discrepancy of MP loads between two studies also suggests that high MP numerical concentrations do not necessarily mean that high MP mass. In our study, the average MP mass (0.000033 g/particle) was generated by weighing selected fibrous and fragmented particles together, which might lead bias on the mean weight due to the mass disparity of two types of MP. To improve the estimation of plastic loads into the ocean from rivers, the mass of fibers and fragments should be individually measured and reported, supplementing the traditional method of reporting plastic numbers.

However, our plastic load estimate also exhibits some uncertainties. Inside the CE, surface MP abundance was influenced by the water density stratification. During February and May, the salty ocean water intrudes into the CE (Xue et al., 2009). When tidal velocity is small, strong density stratification is formed inside the estuary, thus making the mixed layer depth shallower. This causes MP to be concentrated in the upper mixed layer, and thus higher MP abundances are observed under the strong stratification condition. When tidal velocity is large, stratification becomes weaker due to strong mixing. MP may distribute through the depth of the sampling station. MP abundances under the weak stratification condition are lower. As shown in Fig. 8, during February and May, MP abundances in the CE increased as the stratification became stronger (Fig. 8). Due to high river discharge in July, salt intrusion inside the CE was much more limited and the water at the observed stations was largely uninfluenced by the salt water intrusion from the ocean, and thus the water column at the observed stations was well mixed ($\Delta\rho = 0.1$ kg/m^3 at all stations). Therefore, the impacts of stratification on the vertical distribution of MP during July are negligible. In conclusion, the surface MP abundances may be influenced by the stratification strength inside the estuary, especially when the water is well-mixed, and MP may distribute throughout the depth of the sampling station. If we calculate the plastic mass passing the estuary only through the data at the surface, errors may occur. Additionally, tidal action within the estuaries could lead to a mixing of plastic debris that derive either from the river or from the sea (Sadri and Thompson, 2014; Schmidt et al., 2017a,b). The CE is a semi-diurnal mesotidal estuary with a mean tide range of 2.66 m. Hence, the effect of tides on the plastic load should not be neglected. To counteract tidal effects, those datasets from estuaries were excluded in the model by Schmidt et al. (2017a), when they estimated the plastic loads from rivers to the sea. However, the last station (Datong) at the Changjiang River which are not tidally influenced is located about 620 km from the river mouth and upstream from one of the most economically developed and densely inhabited areas of China (Gao et al., 2012). A positive relationship has been found between measures of urban intensity (e.g., population density and urban development) and plastic pollution levels in rivers (Xiong et al., 2019). Moreover, Xiong et al. (2019) found that a considerable amount of microplastics generated in large river catchments are not delivered to the sea. To offset tidal effects, we simply assume that only half the time the tide is pushing litter out into the marine environment in the CE. Hence the plastic load was divided by '2', which was used by van der Wal et al. (2015), who estiamted the plastic flux of european rivers. Finally, the annual MP load, ranging from 268.8 to 453.0 tons, was estimated in our study. It should be noted that this assumption is over simplification. In light of these, an optimum sampling strategy should be built in the further. For instance, plastic samplings within the estuaries over tidal cycles and hydrodynamic measurements are conducted simultaneously, which could generate the estimations free of the tidal effects (Gao et al., 2008). Additionally, long-term continuous observations covering the surface, middle depth, and bottom of the sampling stations should be performed, which would more accurately quantify the MP riverine transport process and the influence of physical processes, thus improving our understanding of the role of rivers in delivering inland plastic debris to the ocean.

4. Conclusions

The role of rivers as a major transport pathway for all sizes of plastic debris generated inland to the marine environment is of

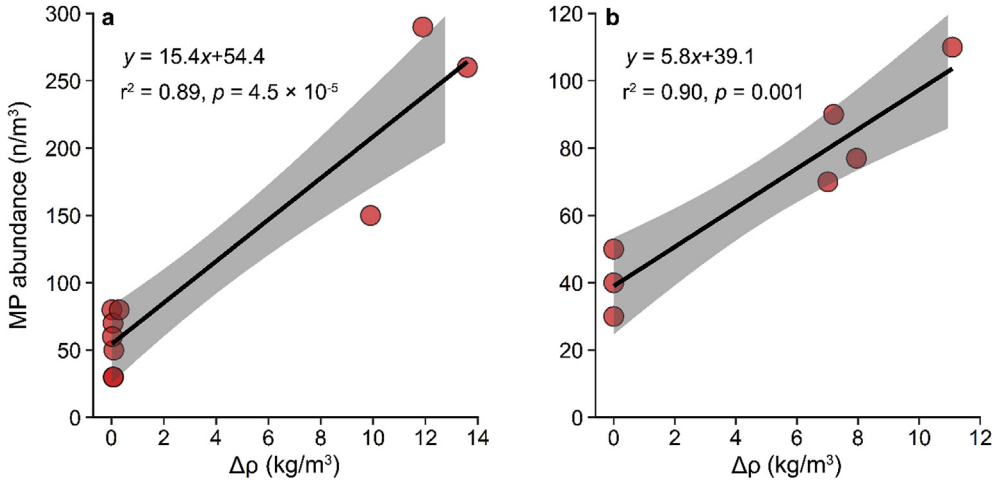

Fig. 8. Relationship between the strength ($\Delta\rho$) of stratification and MP abundance in the CE (a. February, b. May). Gray shading represents the upper and lower 95% confidence interval for the linear model.

increasing ecological concern and is widely recognized (Lebreton et al., 2017; Schmidt et al., 2017a; Siegfried et al., 2017). The Changjiang River, as one of the largest rivers worldwide, has been ranked as the largest plastic waste-contributing catchment to the marine environment (Lebreton et al., 2017; Schmidt et al., 2017a). Based on an intensive sampling of the surface waters in the CE and ECS, the spatial and temporal patterns of MP were studied. Distinct seasonal variations in MP abundances in the studied regions were detected, which was probably caused by the higher rainfall in the wet season. Patchy distributions of floating MP were observed in the ECS in all months. Seasonality in the mean size of MP across the sampling regions was also observed. Mean size in May was apparently smaller than that in February and July. Large temporal variations suggest that the estimates of riverine plastic to the sea may be biased if studies are conducted only during the wet or dry season. The distinctly lower MP mass (0.000033 g/particle) suggested that MP fluxes in previous studies (Lebreton et al., 2017; Schmidt et al., 2017a) were overestimated, and the measurements of MP mass should be included in the further research. Without considering tidal effects, 16–20 trillion MP particles, weighing 537.6–905.9 tons flow through the surface layer (around 30 cm depth) of the CE annually. For more reasonable plastic flux of the world's rivers, standardized monitoring methods, high sampling resolution at spatial and temporal scales as well as the hydrodynamic data should be collected for studying plastic contamination in rivers.

Conflicts of interest

Please check the following as appropriate:

- All authors have participated in (a) conception and design, or analysis and interpretation of the data; (b) drafting the article or revising it critically for important intellectual content; and (c) approval of the final version.
  - •This manuscript has not been submitted to, nor is under review at, another journal or other publishing venue.
  - •The authors have no affiliation with any organization with a direct or indirect financial interest in the subject matter discussed in the manuscript
  - •The following authors have affiliations with organizations with direct or indirect financial interest in the subject matter discussed in the manuscript:

Acknowledgement

Thanks to Shuzhen Song for help in ploting Figure 3. We also appreciate the help from the crew on the R/V Runjiang-1. This study was supported by National Key Research and Development project (2016YFC1402201), the National Natural Science Fund of China (41806137 and 41706002), the State Key Laboratory of Estuarine and Coastal Research of China (2017RCDW05), the Natural Science Foundation of Jiangsu Province (BK20170864), and the International Postdoctoral Exchange Fellowship (20170031) to SZ.

Appendix A. Supplementary data

Supplementary data to this article can be found online at https://doi.org/10.1016/j.watres.2019.06.019.

References

Andrady, A.L., 2011. Microplastics in the marine environment. Mar. Pollut. Bull. 62 (8), 1596–1605.
Bai, M., Zhao, S., Peng, G., Gao, L., Li, D., 2018. Occurrence, characteristics of microplastic during urban sewage treatment process. China Environ. Sci. 38 (5), 1734–1743 (in Chinese).
Boucher, J., Friot, D., 2017. Primary Microplastics in the Oceans: a Global Evaluation of Sources. IUCN Gland, Switzerland.
Browne, M.A., Crump, P., Niven, S.J., Teuten, E., Tonkin, A., Galloway, T., Thompson, R., 2011. Accumulation of microplastic on shorelines woldwide: sources and sinks. Environ. Sci. Technol. 45 (21), 9175–9179.
Cai, M., He, H., Liu, M., Li, S., Tang, G., Wang, W., Huang, P., Wei, G., Lin, Y., Chen, B., 2018. Lost but can't be neglected: huge quantities of small microplastics hide in the South China Sea. Sci. Total Environ. 633, 1206–1216.
Claessens, M., De Meester, S., Van Landuyt, L., De Clerck, K., Janssen, C.R., 2011. Occurrence and distribution of microplastics in marine sediments along the Belgian coast. Mar. Pollut. Bull. 62 (10), 2199–2204.
Cózar, A., Echevarría, F., González-Gordillo, J.I., Irigoien, X., Úbeda, B., Hernández-León, S., Palma, Á.T., Navarro, S., García-de-Lomas, J., Ruiz, A., 2014. Plastic debris in the open ocean. Proc. Natl. Acad. Sci. Unit. States Am. 111 (28), 10239–10244.
Dauvergne, P., 2018. Why is the global governance of plastic failing the oceans? Glob. Environ. Chang. 51, 22–31.
Di Mauro, R., Kupchik, M.J., Benfield, M.C., 2017. Abundant plankton-sized microplastic particles in shelf waters of the northern Gulf of Mexico. Environ. Pollut. 230, 798–809.
Dris, R., Gasperi, J., Rocher, V., Saad, M., Renault, N., Tassin, B., 2015. Microplastic contamination in an urban area: a case study in Greater Paris. Environ. Chem. 12 (5), 592–599.
Dris, R., Gasperi, J., Saad, M., Mirande, C., Tassin, B., 2016. Synthetic fibers in atmospheric fallout: a source of microplastics in the environment? Mar. Pollut. Bull. 104 (1–2), 290–293.
Enders, K., Lenz, R., Stedmon, C.A., Nielsen, T.G., 2015. Abundance, size and polymer composition of marine microplastics≥ 10 μm in the Atlantic Ocean and their modelled vertical distribution. Mar. Pollut. Bull. 100 (1), 70–81.

Eriksen, M., Mason, S., Wilson, S., Box, C., Zellers, A., Edwards, W., Farley, H., Amato, S., 2013. Microplastic pollution in the surface waters of the laurentian great lakes. Mar. Pollut. Bull. 77 (1–2), 177–182.
Eriksen, M., Lebreton, L.C., Carson, H.S., Thiel, M., Moore, C.J., Borerro, J.C., Galgani, F., Ryan, P.G., Reisser, J., 2014. Plastic pollution in the world's oceans: more than 5 trillion plastic pieces weighing over 250,000 tons afloat at sea. PLoS One 9 (12), e111913.
Fazey, F.M., Ryan, P.G., 2016. Biofouling on buoyant marine plastics: an experimental study into the effect of size on surface longevity. Environ. Pollut. 210, 354–360.
Gallagher, A., Rees, A., Rowe, R., Stevens, J., Wright, P., 2016. Microplastics in the Solent estuarine complex, UK: an initial assessment. Mar. Pollut. Bull. 102 (2), 243–249.
Galloway, T., Lewis, C., 2017. Marine microplastics. Curr. Biol. 27 (11), R445–R446.
Gao, L., Li, D., Ding, P., 2008. Nutrient budgets averaged over tidal cycles off the Changjiang (Yangtze River) estuary. Estuar. Estuarine, Coastal and Shelf Science 77 (3), 331–336.
Gao, L., Li, D., Zhang, Y., 2012. Nutrients and particulate organic matter discharged by the Changjiang (Yangtze River): seasonal variations and temporal trends. J. Geophys. Res. 117 (G4), G04001.
Geyer, R., Jambeck, J.R., Law, K.L., 2017. Production, use, and fate of all plastics ever made. Science advances 3 (7), e1700782.
Goldstein, M.C., Titmus, A.J., Ford, M., 2013. Scales of spatial heterogeneity of plastic marine debris in the northeast Pacific Ocean. PLoS One 8 (11), e80020.
Gray, A.D., Wertz, H., Leads, R.R., Weinstein, J.E., 2018. Microplastic in two South Carolina Estuaries: occurrence, distribution, and composition. Mar. Pollut. Bull. 128, 223–233.
Gündoğdu, S., Çevik, C., Ayat, B., Aydoğan, B., Karaca, S., 2018. How microplastics quantities increase with flood events? An example from Mersin Bay NE Levantine coast of Turkey. Environ. Pollut. 239, 342–350.
Hansen, L., 2016. Macro and Micro Plastics in an Urbanized and Non-urbanized Fjord Estuary in the Northeast Pacific Ocean.
Hernandez, E., Nowack, B., Mitrano, D.M., 2017. Polyester textiles as a source of microplastics from households: a mechanistic study to understand microfiber release during washing. Environ. Sci. Technol. 51 (12), 7036–7046.
Hidalgo-Ruz, V., Gutow, L., Thompson, R.C., Thiel, M., 2012. Microplastics in the marine environment: a review of the methods used for identification and quantification. Environ. Sci. Technol. 46 (6), 3060–3075.
Lahens, L., Strady, E., Kieu-Le, T.-C., Dris, R., Boukerma, K., Rinnert, E., Gasperi, J., Tassin, B., 2018. Macroplastic and microplastic contamination assessment of a tropical river (Saigon River, Vietnam) transversed by a developing megacity. Environ. Pollut. 236, 661–671.
Lebreton, L.C., Van der Zwet, J., Damsteeg, J.-W., Slat, B., Andrady, A., Reisser, J., 2017. River plastic emissions to the world's oceans. Nat. Commun. 8, 15611.
Lebreton, L., Slat, B., Ferrari, F., Sainte-Rose, B., Aitken, J., Marthouse, R., Hajbane, S., Cunsolo, S., Schwarz, A., Levivier, A., 2018. Evidence that the great pacific garbage patch is rapidly accumulating plastic. Sci. Rep. 8 (1), 4666.
Liebezeit, G., Dubaish, F., 2012. Microplastics in beaches of the East Frisian islands spiekeroog and kachelotplate. Bull. Environ. Contam. Toxicol. 89 (1), 213–217.
Lima, A., Costa, M., Barletta, M., 2014. Distribution patterns of microplastics within the plankton of a tropical estuary. Environ. Res. 132, 146–155.
Löder, M.G.J., Kuczera, M., Mintenig, S., Lorenz, C., Gerdts, G., 2015. Focal plane array detector-based micro-Fourier-transform infrared imaging for the analysis of microplastics in environmental samples. Environ. Chem. 12 (5), 563–581.
Luo, W., Su, L., Craig, N.J., Du, F., Wu, C., Shi, H., 2019. Comparison of microplastic pollution in different water bodies from urban creeks to coastal waters. Environ. Pollut. 246, 174–182.
Lusher, A.L., Burke, A., O'Connor, I., Officer, R., 2014. Microplastic pollution in the Northeast Atlantic Ocean: validated and opportunistic sampling. Mar. Pollut. Bull. 88 (1–2), 325–333.
Miller, R.Z., Watts, A.J., Winslow, B.O., Galloway, T.S., Barrows, A.P., 2017. Mountains to the sea: river study of plastic and non-plastic microfiber pollution in the northeast USA. Mar. Pollut. Bull. 124 (1), 245–251.
Moore, C.J., Moore, S.L., Weisberg, S.B., Lattin, G.L., Zellers, A.F., 2002. A comparison of neustonic plastic and zooplankton abundance in southern California's coastal waters. Mar. Pollut. Bull. 44 (10), 1035–1038.
Napper, I.E., Thompson, R.C., 2016. Release of synthetic microplastic plastic fibres from domestic washing machines: effects of fabric type and washing conditions. Mar. Pollut. Bull. 112 (1–2), 39–45.
Napper, I.E., Bakir, A., Rowland, S.J., Thompson, R.C., 2015. Characterisation, quantity and sorptive properties of microplastics extracted from cosmetics. Mar. Pollut. Bull. 99 (1–2), 178–185.
Neufeld, L., Stassen, F., Sheppard, R., Gilman, T., 2016. The New Plastics Economy: Rethinking the Future of Plastics.
Ng, K., Obbard, J., 2006. Prevalence of microplastics in Singapore's coastal marine environment. Mar. Pollut. Bull. 52 (7), 761–767.
Nor, N.H.M., Obbard, J.P., 2014. Microplastics in Singapore's coastal mangrove ecosystems. Mar. Pollut. Bull. 79 (1–2), 278–283.
Norén, F., 2007. Small Plastic Particles in Coastal Swedish Waters. KIMO Sweden.
Pedrotti, M.L., Petit, S., Elineau, A., Bruzaud, S., Crebassa, J.-C., Dumontet, B., Martí, E., Gorsky, G., Cózar, A., 2016. Changes in the floating plastic pollution of the Mediterranean Sea in relation to the distance to land. PLoS One 11 (8), e0161581.
Peng, G., Zhu, B., Yang, D., Su, L., Shi, H., Li, D., 2017. Microplastics in sediments of the Changjiang estuary, China. Environ. Pollut. 225, 283–290.
Peng, G., Xu, P., Zhu, B., Bai, M., Li, D., 2018. Microplastics in freshwater river sediments in Shanghai, China: a case study of risk assessment in mega-cities. Environ. Pollut. 234, 448–456.
Rech, S., Macaya-Caquilpán, V., Pantoja, J., Rivadeneira, M., Madariaga, D.J., Thiel, M., 2014. Rivers as a source of marine litter—a study from the SE Pacific. Mar. Pollut. Bull. 82 (1–2), 66–75.
Sadri, S., Thompson, R., 2014. On the quantity and composition of floating plastic debris entering and leaving the Tamar Estuary, Southwest England. Mar. Pollut. Bull. 81 (1), 55–60.
Sala, A., Lucchetti, A., Sartor, P., 2018. Technical solutions for European small-scale driftnets. Mar. Policy 94, 247–255.
Schmidt, C., Krauth, T., Wagner, S., 2017a. Export of plastic debris by rivers into the sea. Environ. Sci. Technol. 51 (21), 12246–12253.
Schmidt, N., Thibault, D., Galgani, F., Paluselli, A., Sempéré, R., 2017b. Occurrence of microplastics in surface waters of the Gulf of lion (NW mediterranean sea). Prog. Oceanogr. 163, 214–220.
Setälä, O., Magnusson, K., Lehtiniemi, M., Norén, F., 2016. Distribution and abundance of surface water microlitter in the Baltic Sea: a comparison of two sampling methods. Mar. Pollut. Bull. 110 (1), 177–183.
Shanghai Statistical Yearbook, 2016. http://www.stats-sh.gov.cn/html/sjfb/201701/1000339.html.
Sheldon, R., Parsons, T., 1967. A continuous size spectrum for particulate matter in the sea. Journal of the Fisheries Board of Canada 24 (5), 909–915.
Siegfried, M., Koelmans, A.A., Besseling, E., Kroeze, C., 2017. Export of microplastics from land to sea. A modelling approach. Water Res. 127, 249–257.
Song, Y.K., Hong, S.H., Jang, M., Kang, J.-H., Kwon, O.Y., Han, G.M., Shim, W.J., 2014. Large accumulation of micro-sized synthetic polymer particles in the sea surface microlayer. Environ. Sci. Technol. 48 (16), 9014–9021.
Song, Y.K., Hong, S.H., Jang, M., Han, G.M., Shim, W.J., 2015. Occurrence and distribution of microplastics in the sea surface microlayer in Jinhae Bay, South Korea. Arch. Environ. Contam. Toxicol. 69 (3), 279–287.
Tamminga, M., Hengstmann, E., Fischer, E.K., 2018. Microplastic analysis in the South Funen Archipelago, Baltic Sea, implementing manta trawling and bulk sampling. Mar. Pollut. Bull. 128, 601–608.
The Changjiang Water Conservancy Committee, 2017. Yangtze River Sediment Bulletin[M]. Changjiang Press, Wuhan, pp. 16–17 (in Chinese).
Tsang, Y., Mak, C., Liebich, C., Lam, S., Sze, E.T., Chan, K., 2017. Microplastic pollution in the marine waters and sediments of Hong Kong. Mar. Pollut. Bull. 115 (1–2), 20–28.
van der Hal, N., Ariel, A., Angel, D.L., 2017. Exceptionally high abundances of microplastics in the oligotrophic Israeli Mediterranean coastal waters. Mar. Pollut. Bull. 116 (1–2), 151–155.
van der Wal, M., van der Meulen, M., Tweehuijsen, G., Peterlin, M., Palatinus, A., Kovač Viršek, M., 2015. SFRA0025: Identification and Assessment of Riverine Input of (Marine) Litter.
Vianelloa, A., Acrib, F., Aubryb, F.B., Boldrinb, A., Camattib, E., Da Rosa, L., Marcetac, T., Moschinob, V., 2015. Occurrence and Distribution of Floating Microplastics in the North Adriatic Sea: Preliminary Results. MICRO2015 29.
Xiong, X., Wu, C., Elser, J., Mei, Z., Hao, Y., 2019. Occurrence and fate of microplastic debris in middle and lower reaches of the Yangtze River – from inland to the sea. Sci. Total Environ. 659, 66–73.
Xu, P., Peng, G., Su, L., Gao, Y., Gao, L., Li, D., 2018. Microplastic risk assessment in surface waters: a case study in the Changjiang Estuary, China. Mar. Pollut. Bull. 133, 647–654.
Xue, P., Chen, C., Ding, P., Beardsley, R.C., Lin, H., Ge, J., Kong, Y., 2009. Saltwater intrusion into the Changjiang River: A model-guided mechanism study. J. Geophys. Res. Oceans 114. C02006.
Zhao, S., Zhu, L., Wang, T., Li, D., 2014. Suspended microplastics in the surface water of the Yangtze Estuary System, China: first observations on occurrence, distribution. Mar. Pollut. Bull. 86 (1–2), 562–568.
Zhao, S., Zhu, L., Li, D., 2015. Microplastic in three urban estuaries, China. Environ. Pollut. 206, 597–604.
Zhao, S., Zhu, L., Li, D., 2016. Microscopic anthropogenic litter in terrestrial birds from Shanghai, China: not only plastics but also natural fibers. Sci. Total Environ. 550, 1110–1115.
Zhao, S., Danley, M., Ward, J.E., Li, D., Mincer, T.J., 2017. An approach for extraction, characterization and quantitation of microplastic in natural marine snow using Raman microscopy. Analytical Methods 9 (9), 1470–1478.
Zhao, S., Zhu, L., Gao, L., Li, D., 2018. Microplastic Contamination in Aquatic Environments. Elsevier, pp. 27–49.

Update

Water Research

Volume 195, Issue , 1 May 2021, Page

DOI: https://doi.org/10.1016/j.watres.2021.116987

Water Research 195 (2021) 116987

Contents lists available at ScienceDirect

Water Research

journal homepage: www.elsevier.com/locate/watres

Corrigendum to 'Analysis of suspended microplastics in the Changjiang Estuary: Implications for riverine plastic load to the ocean' [Water Res. 161 (2019) 560–569/48672]

Shiye Zhao[a,*], Tao Wang[b], Lixin Zhu[a], Pei Xu[a], Xiaohui Wang[a], Lei Gao[a], Daoji Li[a,*]

[a] State Key Laboratory of Estuarine and Costal Research, East China Normal University, Shanghai 200062, China
[b] College of Oceanography, Hohai University, Nanjing 210029, China

The authors regret that the mass estimates of microplastic in the Spring, Summer, Winter and the Total-high value, shown in Table 1, were incorrect in their original paper. Meanwhile, the estimated annual microplastic loads in the surface layer throughout the orginal paper should be changed from '537.6-905.9' tons to '537.6-668.6' tons. The authors would like to apologise for any inconvenience caused. The corrected Table 1 for this paper can be found here:

Table 1
The yearly microplastic load estimations of Changjiang River in 2017.

Season	MP abundance(n/m^3)	Mean discharge(m^3/month)	Discharge$_{ratio}$	Counts in the season	Mass (ton)
Spring	45.4	741.5×10^9	0.022	2.3×10^{12}	74.1
Summer	122.8	1206.2×10^9	0.021	9.5×10^{12}	314.2
Winter	83.0	396.8×10^9	0.022	2.2×10^{12}	72.5
Fall-low	45.4	798.1×10^9	0.021	2.3×10^{12}	76.9
Fall-midpoint	83.0	798.1×10^9	0.021	4.3×10^{12}	140.5
Fall-high	122.8	798.1×10^9	0.021	6.3×10^{12}	207.9
Total-low				16.3×10^{12}	537.6
Total-median				18.2×10^{12}	601.3
Total-high				20.3×10^{12}	668.6

DOI of original article: 10.1016/j.watres.2019.06.019
* Corresponding authors.
E-mail addresses: shiyezhao@gmail.com (S. Zhao), daojili@sklec.ecnu.edu.cn (D. Li).

https://doi.org/10.1016/j.watres.2021.116987